The EMBO Journal (2011) 30, 2719–2733 | © 2011 European Molecular Biology Organization | All Rights Reserved 0261-4189/11
www.embojournal.org

THE EMBO JOURNAL

The androgen receptor fuels prostate cancer by regulating central metabolism and biosynthesis

Charles E Massie[1], Andy Lynch[1], Antonio Ramos-Montoya[1], Joan Boren[1], Rory Stark[1], Ladan Fazli[2], Anne Warren[3], Helen Scott[1], Basetti Madhu[1], Naomi Sharma[1], Helene Bon[1], Vinny Zecchini[1], Donna-Michelle Smith[1], Gina M DeNicola[1], Nik Mathews[1], Michelle Osborne[1], James Hadfield[1], Stewart MacArthur[1], Boris Adryan[4], Scott K Lyons[1], Kevin M Brindle[1], John Griffiths[1], Martin E Gleave[2], Paul S Rennie[2], David E Neal[1,6] and Ian G Mills[1,5,6,*]

[1]CRUK Cambridge Research Institute, Cambridge, UK, [2]The Vancouver Prostate Centre, Vancouver, British Columbia, Canada, [3]Department of Pathology, Addenbrookes Hospital, Cambridge, UK, [4]Cambridge Systems Biology Centre and Department of Genetics, University of Cambridge, Cambridge, UK and [5]Centre for Molecular Medicine Norway, Nordic European Molecular Biology Laboratory Partnership, University of Oslo, Oslo, Norway

The androgen receptor (AR) is a key regulator of prostate growth and the principal drug target for the treatment of prostate cancer. Previous studies have mapped AR targets and identified some candidates which may contribute to cancer progression, but did not characterize AR biology in an integrated manner. In this study, we took an interdisciplinary approach, integrating detailed genomic studies with metabolomic profiling and identify an anabolic transcriptional network involving AR as the core regulator. Restricting flux through anabolic pathways is an attractive approach to deprive tumours of the building blocks needed to sustain tumour growth. Therefore, we searched for targets of the AR that may contribute to these anabolic processes and could be amenable to therapeutic intervention by virtue of differential expression in prostate tumours. This highlighted calcium/calmodulin-dependent protein kinase kinase 2, which we show is overexpressed in prostate cancer and regulates cancer cell growth via its unexpected role as a hormone-dependent modulator of anabolic metabolism. In conclusion, it is possible to progress from transcriptional studies to a promising therapeutic target by taking an unbiased interdisciplinary approach.

The EMBO Journal (2011) **30,** 2719–2733. doi:10.1038/emboj.2011.158; Published online 20 May 2011
Subject Categories: molecular biology of disease; genomic & computational biology

Keywords: androgen receptor; chromatin; metabolism; prostate cancer; transcription

*Corresponding author. Department of Uro-Oncology, CRUK Cambridge Research Institute, Robinson Way, Cambridge CB2 0RE, UK.
Tel.: +44 122 340 4463; Fax: +44 122 340 4199;
E-mail: ian.mills@cancer.org.uk or ian.mills@ncmm.uio.no
[6]These authors contributed equally to this work

Received: 3 November 2010; accepted: 21 April 2011; published online: 20 May 2011

Introduction

The androgen receptor (AR) is a ligand activated transcription factor and is the main therapeutic target in prostate cancer. Androgen deprivation therapy (chemical castration) is an effective first-line therapy for prostate cancer, but despite good initial responses the recurrence of castrate-resistant disease is common and ultimately fatal. Functional studies have shown that the AR is essential for cell viability, proliferation and invasion in both hormone-sensitive and castrate-resistant prostate cancer (Haag *et al*, 2005; Hara *et al*, 2008; Snoek *et al*, 2009). These findings are supported by clinical studies reporting the sensitivity of castrate-resistant prostate cancer to second-generation AR antagonists and hormone synthesis blockade (Attar *et al*, 2009; Attard *et al*, 2009; Tran *et al*, 2009). In castrate-resistant disease, where tumours are less sensitive to androgen depletion, AR activity is maintained by gene amplification (Visakorpi *et al*, 1995), activating mutations (Veldscholte *et al*, 1990; Steinkamp *et al*, 2009) or signalling cross talk with other oncogenic pathways (Craft *et al*, 1999). All of these mechanisms suggest a strong selective pressure to maintain AR-regulated signalling pathways in castrate-resistant disease, although the nature of these important pathways has remained unclear.

Previous studies have aimed to identify androgen-regulated genes or AR genomic binding sites (Wang *et al*, 2007; Jia *et al*, 2008; Yu *et al*, 2010). However, no single study has identified the transcriptional networks, which underlie AR dependency in both hormone naive and castrate-resistant prostate cancer. Individual studies have focussed on the use of a single model of prostate cancer (LNCaP or its *in vitro*-derived subclones) (Velasco *et al*, 2004; Massie *et al*, 2007; Wang *et al*, 2007, 2009), been limited by genome coverage on microarrays (Massie *et al*, 2007; Wang *et al*, 2007; Jia *et al*, 2008), did not map sites of transcriptional activity (Massie *et al*, 2007; Wang *et al*, 2009) or assessed only a limited number of time points following androgen stimulation (Velasco *et al*, 2004). These studies have provided important insights into the upstream mechanisms which direct the transcriptional activities of the AR and identified a number of transcription factors which cooperate with or antagonize AR activity (Wang *et al*, 2007; Jia *et al*, 2008; Yu *et al*, 2010). However, efforts to identify the key downstream targets of the AR in prostate cancer have identified indirect links to anabolic pathways (Heemers *et al*, 2001, 2004; Xu *et al*, 2006) or focussed on cell-cycle regulators (Knudsen *et al*, 1998; Wang *et al*, 2009), some of which appear only to be AR targets in models of castrate-resistant prostate cancer (Wang *et al*, 2009). Therefore, a detailed

map of AR-regulated genes in diverse models of prostate cancer is needed to better understand the essential signalling pathways downstream of the AR in both hormone-sensitive and castrate-resistant stages of the disease.

Results

Identifying a core set of direct AR-regulated genes

To identify direct AR-regulated genes, we combined genome-wide AR binding profiles with detailed transcript profiling. We also integrated androgen-stimulated recruitment of the transcriptional machinery to identify a core set of AR binding sites, which regulate gene expression in prostate cancer cells. First, we mapped AR binding profiles in two cell lines which represent distinct molecular subtypes of prostate cancer: one harbouring an AR ligand binding domain mutation (LNCaP); one harbouring an AR gene amplification (VCaP). Using chromatin immunoprecipitation with direct Solexa sequencing (ChIP-seq), we identified 11 053 AR binding sites in LNCaP cells and 51 811 androgen-dependent AR binding sites in VCaP cells (Supplementary Tables S1 and S2). VCaP cells harbour a copy number gain of the AR gene locus resulting in elevated AR expression (Supplementary Figure S1; Makkonen *et al*, 2011), which may at least in part explain the larger number of AR binding sites found in VCaP compared with LNCaP cells. Despite the difference in total number of identified binding sites, over 90% of the LNCaP AR binding sites were also found in the VCaP cells (Figure 1A; Supplementary Figure S2; Supplementary Table S3), suggesting that these core binding sites are commonly occupied by the AR even in distinct molecular subtypes of prostate cancer. The common AR binding sites between LNCaP and VCaP cells included all established AR target genes (Figure 1A; Supplementary Figure S2), had significant correlations with other published data sets (Supplementary Figure S3) and identified thousands of AR targets not identified in previous AR ChIP studies (Supplementary Table S3). As a resource we have compiled all published AR ChIP-chip studies together with our data in Supplementary Table S3.

Next, we integrated the location of the transcriptional machinery on the prostate cancer genome together with detailed expression profiling. We identified 15 761 androgen-dependent RNAP II (serine 5 phosphorylated RNA polymerase II) regions in LNCaP cells using ChIP-seq (Supplementary Table S4), 1283 of which overlapped with androgen-stimulated AR binding sites (Figure 1B). The regions enriched for RNAP II alone ($n = 14\,478$) represent sites of paused, primed or active transcription (Bernstein *et al*, 2006; Core *et al*, 2008); however, sites to which the AR and RNAP II are dynamically co-recruited ($n = 1283$) are candidate regions for androgen-stimulated transcriptional initiation (explored in detail below). Using Illumina BeadArrays, we made a detailed study of androgen-regulated gene expression with samples taken every 30 min for 4 h and then every hour up to 24 h following androgen stimulation of LNCaP cells. This detailed expression array time course made it possible to identify androgen-regulated gene expression changes based on trends with time following androgen stimulation (using autocorrelation), allowing detection of early and even small gene expression changes (see Materials and methods for details). In total, we found 3319 transcripts with altered expression in response to androgens, 1556 (47%) transcripts were upregulated and 1763 (53%) were downregulated (Supplementary Table S5).

We made a combined analysis of our treatment contrast ChIP and detailed gene expression profiling to identify AR binding sites which recruit the transcriptional machinery and direct AR-regulated genes. Such combined analyses require a predefined genomic distance between transcript factor binding sites and genes, which is often set arbitrarily. To address this issue, we took a more empirical approach using gene set enrichment analysis (GSEA) to define the optimal genomic distance between AR binding sites (peaks) and androgen-regulated genes (gene boundaries). We found that genes located within 25 kb of an AR binding site were the most significantly enriched for androgen-regulated genes; the maximal enrichment score at 25 kb suggests that smaller genomic windows would include a greater proportion of false negatives and that larger genomic windows would include a greater proportion of false positives (Figure 1C; Supplementary Figure S3; Supplementary data). Therefore, using this 25 kb window we integrated the genomic locations of AR binding sites, androgen-stimulated recruitment of the core transcriptional machinery and detailed gene expression profiling (Figure 1D). This integrated analysis revealed that loci bound by either the AR or RNAP II alone contain genes which are upregulated, downregulated or not affected by AR signalling (Figure 1D). This finding is consistent with previous studies showing that the AR can directly activate or repress transcription (Margiotti *et al*, 2007; Prescott *et al*, 2007), that only a proportion of transcription factor binding sites are active in a given cellular context (Carroll *et al*, 2006) and that RNAP II enriched regions of the genome include both sites of active transcription and also sites where transcription has paused or stalled (Bernstein *et al*, 2006; Core *et al*, 2008). In contrast, the core overlap of androgen-stimulated AR binding sites and RNAP II recruitment showed specific enrichment for androgen upregulated transcripts (Figure 1D). Therefore, our combined analysis has identified a core set of AR binding sites that recruit the transcriptional machinery and upregulate the transcription of adjacent genes. These core AR targets may help to identify the features of transcriptionally active AR binding sites.

Analysis of the genomic sequences underlying all AR binding sites found in LNCaP, VCaP or those identified in both cell lines revealed evolutionary conservation, enrichment of AR binding sequences and motifs for previously reported AR interacting transcription factors, including forkhead and NF-1 (Supplementary Figure S1; Supplementary Table S6) (Wang *et al*, 2007; Jia *et al*, 2008). The overlapping AR and RNAP II sites showed significant enrichment of 6 bp and 15 bp AR binding motifs (Figure 1E and F), but also showed enrichment for CREB and AHR binding motifs, in contrast to the full set of AR binding sites (Supplementary Figure S1; Supplementary Table S6). *De novo* motif analysis revealed an inverted-repeat 15 bp ARE similar to the *in vitro*-derived consensus binding motif (Roche *et al*, 1992) and also a 6 bp motif consisting of one half of the consensus 15 bp element, as previously reported in other AR ChIP studies (Massie *et al*, 2007; Wang *et al*, 2007) (Figure 1E; Supplementary Figure S1).

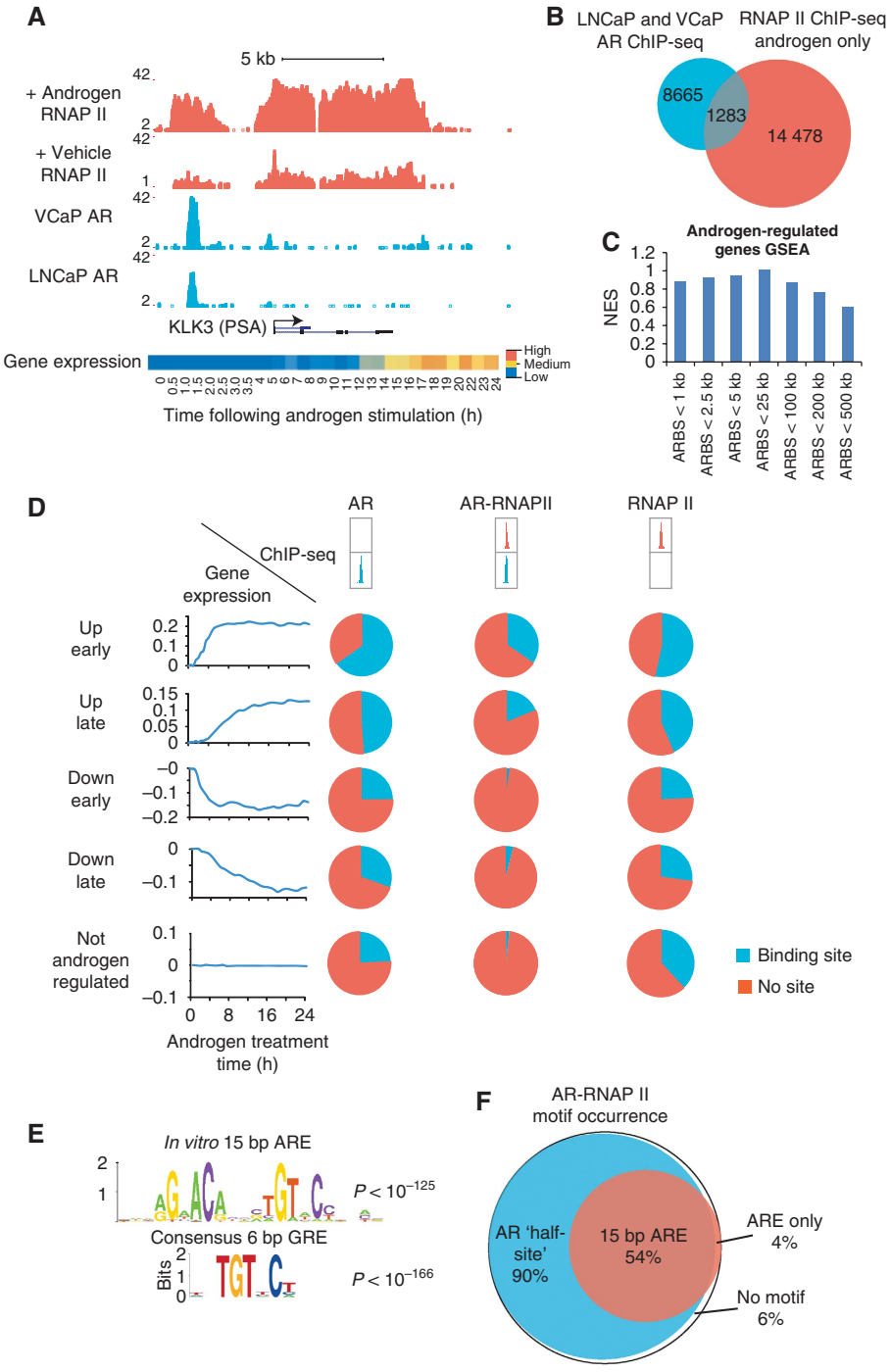

Figure 1 Mapping transcriptional targets of the AR. (**A**) ChIP-seq enrichment profiles for AR and RNAP II with or without androgen treatment and in LNCaP or VCaP cells, as indicated (cells cultured in steroid depleted media and treated with 1 nM R1881 or 0.01% ethanol for 4 h). Location of the PSA gene is indicated below enrichment plots, arrow indicates the direction of transcription. Androgen-stimulated expression is shown at the bottom, represented as a heatmap showing expression changes with time following androgen stimulation (1 nM R1881, data from Illumina beadarray gene expression time course). (**B**) Venn diagram showing the overlap between AR binding sites and androgen-dependent RNAP II enriched genomic regions (1 nM R1881, 4 h; data from intersects of all peaks overlapping by >1 bp). (**C**) Gene set enrichment analysis (GSEA) of androgen-regulated genes (Illumina beadarray androgen stimulation time course), using gene sets identified within genomic windows from 1 to 500 kb from AR binding sites. (**D**) Combined analysis of AR binding sites, androgen-dependent RNAP II enriched regions and androgen-regulated genes. Genes are grouped by expression changes early (<4 h), late (>4 h), up, down or no change in response to androgen stimulation (left). Pie charts indicate the proportion of genes with adjacent AR, RNAP II or overlapping AR-RNAP II sites in each set (<25 kb from gene boundaries; groups indicated above). (**E**) Sequence logos for 15 and 6 bp AR/GR binding motifs (*P*-values indicate enrichment in AR-RNAP II overlapping regions). (**F**) Venn diagram showing the occurrence of 15 and 6 bp AR binding motifs in androgen-dependent AR-RNAP II overlapping sites.

Identifying cellular processes regulated by the AR

Our combined analysis of AR, RNAP II and detailed expression profiling also identified a core set of direct androgen-regulated genes for further investigation. We defined direct AR targets as those genes induced by androgen treatment and for which there were overlapping hormone-induced AR binding sites

within 25 kb of the genes. This definition identified a sufficient number of genes to allow pathway enrichment analysis and as a resource we have included a table noting these genes together with their androgen-stimulated expression profile, annotated with the location of adjacent AR and RNAP II binding sites (Supplementary Table S7). Interestingly, this core set of direct AR-regulated genes gave overlapping but distinct functional enrichment by gene ontology (GO) analysis compared with gene expression data alone (Figure 2A; Supplementary Tables S8 and S9).

While many established classes of AR target gene were represented within the data sets as a whole, including cell-cycle regulators (e.g., CDC25, CDK6 and E2F1) and signalling molecules which have been implicated in prostate cancer (e.g., WWP1, ERBB2, MEK5, SGK1 and IGF1R) (Figure 2C; Craft *et al*, 1999; Hellawell *et al*, 2002; Mehta *et al*, 2003; Chen *et al*, 2007; Sherk *et al*, 2008), the combined analysis of direct AR targets and androgen-regulated genes also revealed a significant enrichment of metabolic targets (Figure 2A–C; Supplementary Table S9). GO analysis highlighted central metabolism and biosynthetic pathways among the direct AR targets (Figure 2A) and GSEA also revealed significant enrichment of central metabolism and metabolic gene signatures (Mootha *et al*, 2003) among direct AR-regulated genes (Figure 2B). Unlike other biological processes, metabolism has been subjected to decades of detailed biochemical study and consists of a series of interlinked and well-characterized processing steps. This makes the functional consequences of changes in enzyme expression uniquely predictable for metabolic pathways and made these pathways an ideal testing ground for the linkages established by our genomics data. We found that the AR directly upregulated expression of key steps in glucose uptake and glycolysis including glucose transporter 1 (GLUT1/SLC2A1), hexokinase I and II (HK1 and HK2), phosphofructokinase (PFK2/PFKFB2) and also many anabolic enzymes at both the transcript and protein level (Figure 2C and D; Supplementary Figures S4 and S5). Based on the annotation of these direct metabolic AR target genes within well-defined metabolic pathways we predicted that the AR may facilitate cell growth by promoting glucose uptake and anabolic metabolism (Figure 2D). To test these predictions from our genomics data, we undertook comprehensive metabolomic profiling to assess the effects of AR signalling on glucose consumption and lactate production, O_2 consumption and detailed metabolite profiling of intracellular and extracellular metabolites using proton nuclear magnetic resonance (1H NMR) and glucose flux using carbon-13-labelled glucose with gas chromatography–mass spectrometry (GC/MS).

The AR regulates aerobic glycolysis and anabolism in prostate cancer cells

Androgen stimulation of prostate cancer cells increased glucose uptake and increased lactate production in normoxia, but had no effect on oxygen consumption, showing that AR signalling does indeed stimulate aerobic glycolysis (Christofk *et al*, 2008; Vander Heiden *et al*, 2009) (Figure 2E–I; Supplementary Figure S4F). Citrate levels were also increased following androgen stimulation (Figure 2G) while the levels of the tricarboxylic acid (TCA) cycle metabolite succinate remained unchanged (Figure 2H), further underscoring androgen stimulation of glycolysis and highlighting the truncated TCA cycle in prostate epithelial cells (Costello *et al*, 1997). We also found that AR signalling significantly stimulated anabolic synthesis, by measuring the flux from carbon-13-labelled glucose to amino acids (e.g., glutamine) and RNA (ribose) in response to androgen stimulation (Supplementary Figure S6; Figure 4F and G). Therefore by specifically upregulating these rate-limiting steps in glycolysis, the AR stimulates energy production and provides carbon needed for macromolecule synthesis. In addition, we found that the AR stimulated the expression of key anabolic enzymes, which utilize glucose metabolites (e.g., fatty acid synthase (FASN) and acetyl-CoA carboxylase α (ACACA)) and master regulators of biosynthesis (e.g., MTOR, encoded by FRAP1; Supplementary Figure S5). Therefore, AR signalling appears to coordinately regulate energy production and biosynthesis at multiple levels (Figure 2D), highlighting these metabolic pathways as potential targets to inhibit the growth of prostate cancer cells (Migita *et al*, 2009).

CAMKK2 is a metabolic master regulator downstream of the AR in prostate cancer cells

Identifying cancer-specific alterations that affect central metabolism is a major challenge for drug discovery in cancer biology. Therefore, we used clinical gene expression data (Rhodes *et al*, 2004) to assess cancer-specific expression of AR targets (Supplementary Table S7). Among the direct AR target genes, we identified calcium/calmodulin-dependent kinase kinase 2 (CAMKK2, Figure 3A) as consistently overexpressed in prostate cancer in nine independent clinical gene expression studies (Rhodes *et al*, 2004; Varambally *et al*, 2005), showing a similar pattern to the established prostate cancer marker AMACR (Jiang *et al*, 2001, 2002) (Figure 3B; Supplementary Figure S5). CAMKK2 was only highlighted by integrating AR genomic targets with clinical expression data, since we identified a core set of 1164 direct AR-regulated genes and on average CAMKK2 was ranked only 40th over the nine clinical studies (Figure 3B). CAMKK2 has

Figure 2 Functional annotation of direct AR-regulated genes. (**A**) Gene ontology (GO) network of direct AR-regulated genes (androgen upregulated genes within 25 kb of AR binding site, Cytoscape BiNGO analysis). (**B**) Gene set enrichment analysis (GSEA) plots for direct AR-regulated genes, showing enrichment for carbohydrate metabolism GO and the curated peroxisome proliferator-activated receptor γ co-activator 1-α (PPARGC1A) metabolic gene set. (**C**) Gene expression heatmaps, showing androgen-regulated genes within 25 kb of an AR binding site, grouped by functional categories (indicated above; data from Illumina beadarray time course in LNCaP cells; pathway annotations from GO annotations, KEGG pathways and literature reviews). (**D**) Schematic showing the locations of direct AR-regulated genes in metabolic and cell-cycle pathways. Red boxes indicate direct AR upregulated genes, blue boxes represent direct AR downregulated genes and yellow boxes indicate proteins not found to be regulated by the AR. Dashed lines indicate intermediate steps not shown. (**E–I**) Levels of (**E**) glucose, (**F**) lactate, (**G**) citrate, (**H**) succinate and (**I**) oxygen consumption rates were measured following growth of LNCaP prostate cancer cells in steroid depleted media with and without androgen stimulation (1 nM R1881). Expressed as μM lactate, μM citrate, μM succinate and % glucose consumption in cell culture media and nmol/ml/min oxygen consumption rate, all normalized to cell number (represented as mean ± s.e.m.; each data point represents triplicate measurements).

previously been linked to central metabolism as an essential regulator of the metabolic sensor AMP kinase (AMPK) in the hypothalamus (Anderson *et al*, 2008), implicating CAMKK2 also as a regulator of cellular metabolism. The AR was recruited to the CAMKK2 promoter in both androgen-dependent and castrate-resistant prostate cancer cell lines

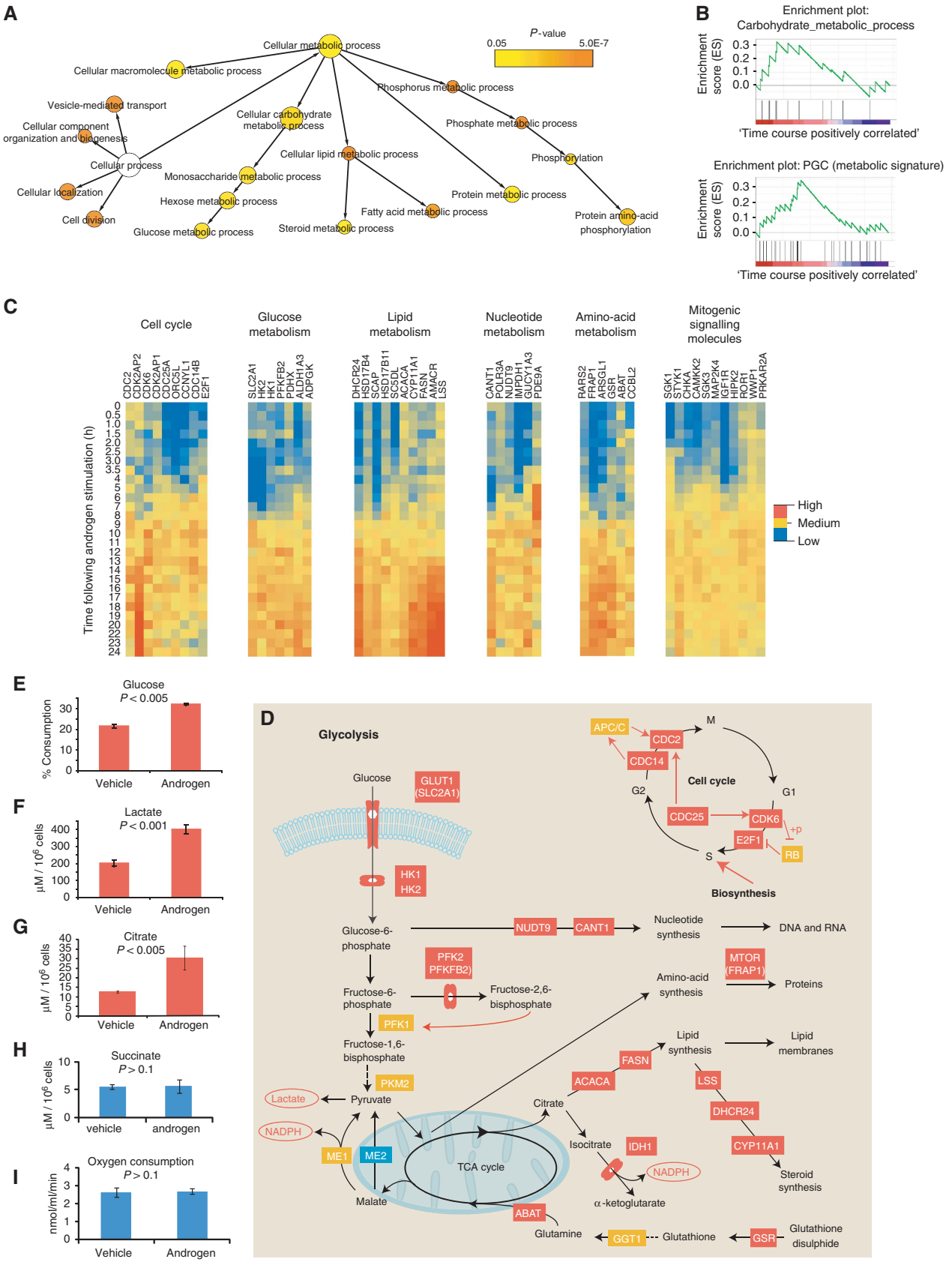

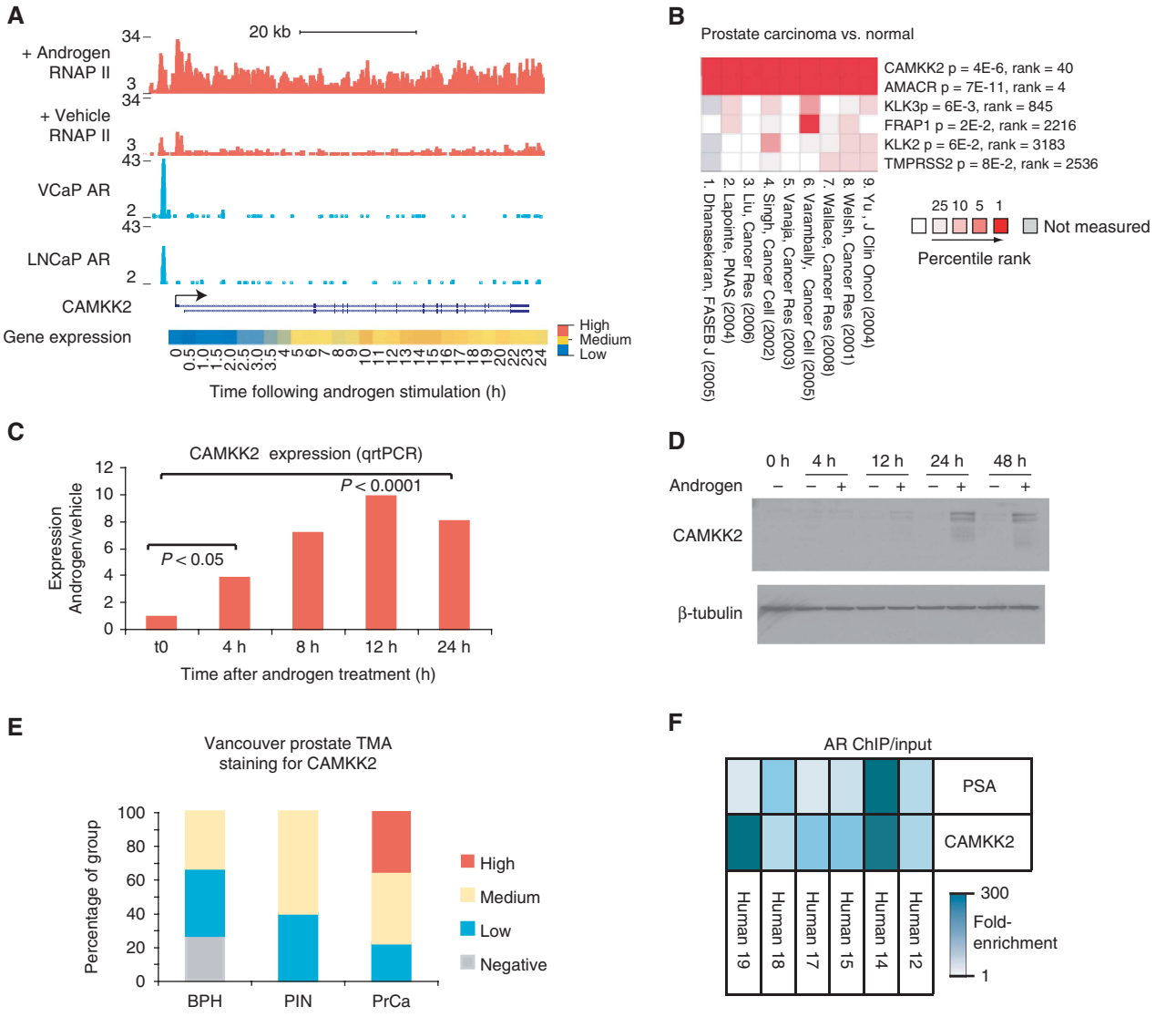

Figure 3 The regulation and expression of CAMKK2 in prostate cancer. (**A**) ChIP-seq enrichment profiles for the AR (LNCaP and VCaP) and RNAP II (LNCaP), as indicated. The CAMKK2 gene position is indicated below, arrow indicates the direction of transcription. Androgen-regulated expression of CAMKK2 is shown in the heatmap below (data from Illumina beadarray time course in LNCaP cells). (**B**) Summary of gene expression data from nine separate studies using clinical samples showing the expression of six direct AR targets in prostate cancer compared with benign (represented as the percentile rank for each gene in each set and labelled with median gene rank and median *P*-value for each gene over all nine studies; data from Oncomine). (**C**) Real-time qrtPCR quantification of CAMKK2 transcript following androgen stimulation (LNCaP cells cultured in steroid depleted media and treated with1 nM R1881; data represented as average of triplicates ± s.e.m.). (**D**) Western blotting for CAMKK2 and β-tubulin, using LNCaP cell lysates harvested following 72 h culture in steroid depleted media followed by treatment with either androgen (1 nM R1881) or vehicle (0.01% ethanol) for 4, 12, 24 or 48 h, as indicated. (**E**) Summary of CAMKK2 immunohistochemical staining of benign (BPH), prostate intraepithelial neoplasia (PIN) and prostate cancer (PrCa) (data from Vancouver prostate tissue microarray, $n = 84$ cores). (**F**) Heatmap showing the results of AR ChIP from six individual clinical prostate cancer samples, with Real-time PCR detection of the CAMKK2 promoter and PSA (KLK3) enhancer regions (represented as fold-enrichment over total input DNA, normalized to unbound control locus).

(Supplementary Figure S7), suggesting that CAMKK2 is an AR target in both stages of the disease. CAMKK2 transcript and protein were upregulated early (<4 and <12 h, respectively) in response to androgen stimulation and downregulated in response to the AR antagonist bicalutamide, underscoring the direct regulation of CAMKK2 by the AR (Figure 3C and D; Supplementary Figure S7i). In clinical samples, we found CAMKK2 protein overexpression in two independent prostate cancer cohorts (Figure 3E; Supplementary Figure S7; Supplementary Table S10) and confirmed that CAMKK2 was a direct AR target in a panel of clinical prostate cancer samples using ChIP from human tissue (Figure 3F). These data highlight CAMKK2 as an AR-regulated gene in prostate cancer and in combination with the published role of CAMKK2 as a metabolic regulator (Anderson *et al*, 2008), prompted us to investigate the functional effects of AR-CAMKK2 signalling.

Since CAMKK2 has been shown to phosphorylate AMP activated kinase (AMPK) in the hypothalamus (Anderson *et al*, 2008) we tested the effects of CAMKK2 inhibition on AMPK phosphorylation in a panel of prostate cancer cell lines. Inhibition of CAMKK2 using siRNA or the specific inhibitor STO-609 (Tokumitsu *et al*, 2002) reduced p-AMPK without affecting total AMPK levels (Figure 4A;

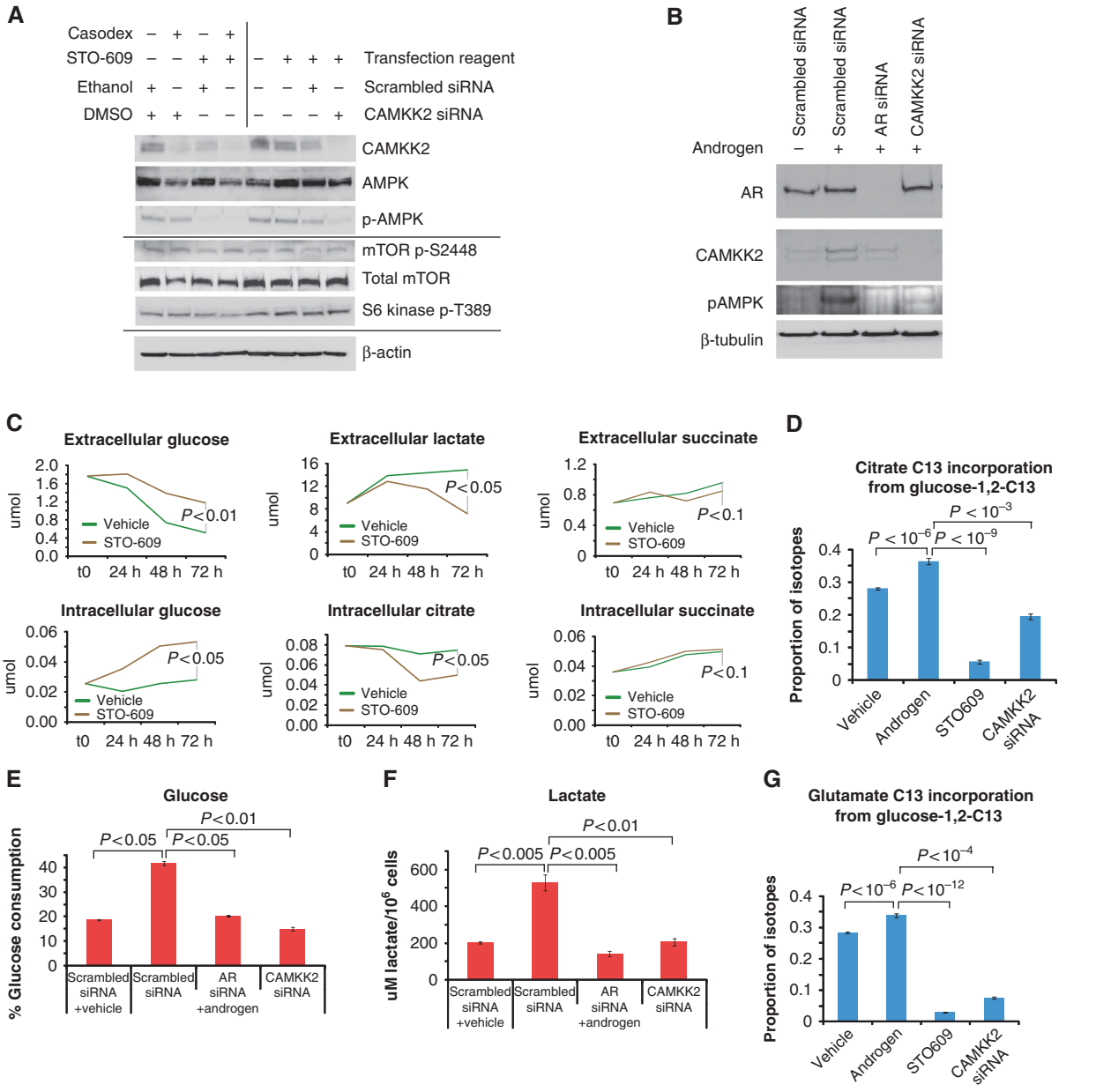

Figure 4 CAMKK2-AMPK signalling and glucose metabolism downstream of the AR in prostate cancer cells. (**A**) Western blotting of lysates from LNCaP cells 72 h following treatment with AR antagonist (casodex), CAMKK2 inhibitor (STO-609), vehicle controls, CAMKK2 siRNA or scrambled control siRNA. (**B**) Western blotting of lysates from LNCaP cells 72 h after transfection of AR siRNA, CAMKK2 siRNA or scrambled control siRNA in the presence and absence of androgens (cells grown in steroid depleted media and treated with 1 nM R1881 or 0.01% ethanol). (**C**) Proton nuclear magnetic resonance (1H NMR) measurements of glucose, lactate and citrate in cell culture media (extracellular) or cell lysates (intracellular) from LNCaP cultures treated with CAMKK2 inhibitor (25 μM STO-609) or vehicle control (0.01% DMSO) for 24, 48 and 72 h, as indicated (average of triplicate experiments, normalized to cell counts). (**D**) Measurement of glucose flux to citrate using carbon-13-labelled glucose (1,2-13C2-glucose) and GC/MS. LNCaP cells were cultured for 72 h in the presence or absence of androgen stimulation (1 nM R1881) and with or without CAMKK2 inhibition (25 mM STO-609) or siRNA knock-down (represented as the proportion of citrate isotopes containing carbon-13; mean of triplicates ± s.e.m.). (**E**, **F**) Extracellular glucose and lactate levels in LNCaP cell culture media 72 h following transfection of AR siRNA, CAMKK2 siRNA or scrambled control siRNA in the presence and absence of androgens (1 nM R1881 or 0.01% ethanol; concentrations measured using enzymatic assays, Abcam). (**G**) Measurement of glucose flux to glutamate using carbon-13-labelled glucose (1,2-13C2-glucose) and GC/MS. LNCaP cells were cultured for 72 h in the presence or absence of androgen (1 nM R1881 or 0.01% ethanol) and with or without CAMKK2 inhibition (25 μM STO-609) or CAMKK2 siRNA knock-down (represented the proportion of glutamate isotopes containing carbon-13; mean of triplicates ± s.e.m.).

Supplementary Figure S8). This shows that CAMKK2 is required for AMPK phosphorylation in prostate cancer cells and confirmed that CAMKK2 was inhibited by the STO-609 compound. Androgen treatment induced AMPK phosphorylation and this was blocked by siRNA knock-down of either the AR or CAMKK2 (Figure 4B), highlighting an AR-CAMKK2-AMPK signalling pathway in prostate cancer cells. AMPK activity promotes glycolysis by phosphorylation of PFK2 and negatively regulates protein synthesis by phosphorylating the TSC1/TSC2 complex upstream of mTOR (Marsin *et al*, 2000; Gwinn *et al*, 2008). We assessed the relative impact of the AR-CAMKK2-AMPK pathway on

mTOR by blotting for phospho-mTOR and for phospho-S6 kinase downstream of mTOR. These surrogates for mTOR activity were unaffected either by STO-609 or by CAMKK2 siRNA, indicating that protein synthesis is unperturbed by targeting the AR-CAMKK2-AMPK (Figure 4A; Supplementary Figure S8). By contrast glycolytic flux was significantly inhibited by these interventions (Figure 4C–E); cells treated with the CAMKK2 inhibitor STO-609 or CAMKK2 siRNA had reduced glucose uptake and produced less lactate and citrate (Figure 4C–F), suggesting a reduction in aerobic glycolysis. In addition, metabolic profiling revealed an intracellular accumulation of glucose following CAMKK2 inhibition (Figure 4C) and decreased anabolism from glucose to citrate, ribose and amino acids (Figure 4G; Supplementary Figure S6), together suggesting a metabolic block downstream of glucose uptake (Figure 5F). CAMKK2 inhibition also reduced PFK activity (Supplementary Figure S8), suggesting that AR-CAMKK2-AMPK signalling may stimulate glucose uptake and glycolysis through effects on PFK (Figure 5F). Importantly, CAMKK2 knock-down or inhibition was sufficient to block AR stimulated glucose uptake and lactate production (Figure 4E and F), highlighting CAMKK2 as an essential regulator of these metabolic effects downstream of the AR in prostate cancer cells.

Both RNAi knock-down and chemical inhibition of CAMKK2 reduced proliferation in prostate cancer cells (Figure 5A;

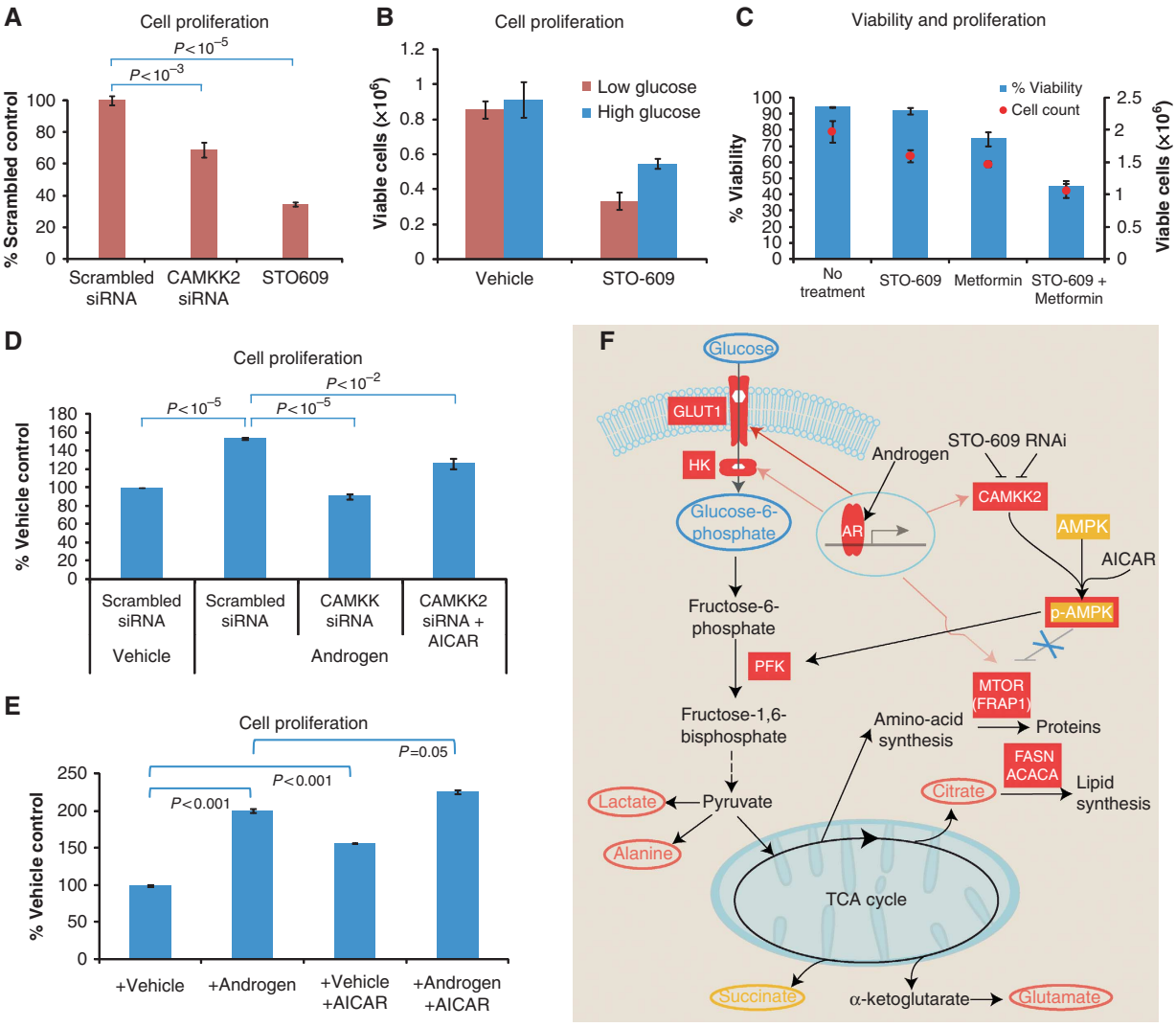

Figure 5 AR-CAMKK2-AMPK signalling is required for AR-stimulated proliferation in prostate cancer cells. (**A**) Cell proliferation of LNCaP cells 120 h following CAMKK2 siRNA transfection or CAMKK2 inhibitor treatment (25 μM STO-609; represented as % no treatment control, average of triplicate MTS assay experiments ± s.e.m.). (**B**) Viable cell counts 72 h following treatment of LNCaP cells with CAMKK2 inhibitor (25 μM STO-609), in low glucose medium (1 g/l) or high glucose medium (4.5 g/l; represented as average of triplicate experiments ± s.e.m.). (**C**) Viable cell counts and percentage viability of LNCaP cells following 72 h treatment with CAMKK2 inhibitor (25 μM STO-609), the anti-diabetes drug metformin (5 mM) or the combination treatment (average of triplicate experiments ± s.e.m.). (**D**) Cell proliferation of LNCaP cells cultured in steroid depleted medium for 120 h following transfection with scrambled siRNA or CAMKK2 siRNA, with or without androgen stimulation (1 nM R1881) or AMPK activation (200 μM AICAR; average of triplicate MTS experiments ± s.e.m.). (**E**) Cell proliferation of LNCaP cells cultured in steroid depleted medium for 120 h and treated with vehicle (0.01% ethanol) or androgen (1 nM R1881) with or without AMPK stimulation (200 μM AICAR; average of triplicate MTS experiments ± s.e.m.). (**F**) Schematic model of AR-CAMKK2 signalling in prostate cancer cells, highlighting the pathways implicated in the stimulation of glycolysis, biosynthesis and proliferation via AMPK (upstream metabolites indicated in blue ovals, downstream metabolites indicated in red ovals and AR-regulated genes indicated by solid red boxes, yellow indicates metabolites and genes showing no detected change).

Supplementary Figure S8), while CAMKK2 overexpression stimulated proliferation (Supplementary Figure S8). Interestingly, combining CAMKK2 inhibition with glucose depletion or the metabolic inhibitor metformin has a synergistic effect on proliferation and cell viability (Figure 5B and C). To assess the contribution of other signalling pathways downstream of CAMKK2 in prostate cancer we used phospho-protein profiler arrays from replicate CAMKK2 siRNA transfected and STO-609-treated cell lysates. These showed almost identical profiles (Pearson's correlation >0.9), highlighting the specificity of STO-609 in this context. Loss of AMPK phosphorylation was confirmed on the phospho-specific antibody array following either CAMKK2 siRNA or STO-609 treatment, interestingly both treatments resulted in loss of AMPK1a phosphorylation but no measurable change in AMPKa2 phosphorylation (Supplementary Figure S9). In addition, we observed no change in the phosphorylation of the CAMK1 and CAMK4 target CREB (Supplementary Figure S9), suggesting no gross alterations in CAMK1 or CAMK4 signalling downstream of CAMKK2 inhibition in AR-dependent prostate cancer cells. To further test the contribution of these downstream targets of CAMKK2, we used siRNA knock-down of CAMK1 and CAMK4, and the AMPK activator AICAR. Knock-down of CAMK1 and CAMK4 had marginal effects on cell proliferation, glucose consumption and lactate production (Supplementary Figure S9). These effects were significantly less than the effects of CAMKK2 inhibition in both androgen-dependent and castrate-resistant cell lines which express the AR (Supplementary Figure S9; Figure 6B). In contrast, the AMPK activator AICAR was sufficient to rescue the growth inhibitory effects of CAMKK2 RNAi knock-down or STO-609 treatment in AR expressing cell lines (Figure 5D; Supplementary Figure S8). Importantly, while CAMKK2 knock-down or chemical inhibition significantly inhibited androgen-stimulated proliferation, the AMPK activator AICAR was sufficient to rescue this effect and also to rescue the growth inhibitory effects of androgen depletion (Figure 5D and E; Supplementary Figure S8). Together, these functional studies implicate CAMKK2-AMPK signalling in prostate cancer growth and place this signalling axis downstream of the AR. Overall, our data suggest that CAMKK2 stimulates glycolysis by activating AMPK and without significant effects on biosynthesis (e.g., mTOR signalling) or other CAMKK2 substrates (Figure 5F).

CAMKK2 is functionally important in hormone-sensitive and castrate-resistant prostate cancer

In clinical samples, CAMKK2 levels were reduced following neoadjuvant hormone therapy, confirming *in vivo* the AR regulation of CAMKK2 (Figure 6A). Interestingly, we found that CAMKK2 levels were increased again in castrate-resistant disease (Figure 6A; Supplementary Table S10). This supports the *in vitro* findings that the AR binds to the CAMKK2 promoter in castrate-resistant prostate cancer cell lines (Supplementary Figure S7i) and that both glycolysis (Supplementary Figure S9) and cell proliferation (Figure 6B; Supplementary Figure S8) were sensitive to CAMKK2 inhibition or knock-down in these resistant cell lines. Collectively, these data implicate CAMKK2 in late stage drug-resistant prostate cancer where existing therapies are no longer effective. Therefore, to assess the functional importance of CAMKK2 in tumour formation we used the C4-2B xenograft model of castrate-resistant prostate cancer, a model which mirrors clinical late stage disease where AR signalling frequently remains functionally important (Snoek *et al*, 2009; Tran *et al*, 2009). Pharmacokinetic measurements showed that the CAMKK2 inhibitor STO-609 had a moderate half-life, low clearance and a low volume of distribution when administered IV or IP (Supplementary Figure S10). There was little difference in the plasma concentration of STO-609 following a single administration and after 19 sequential doses, indicating neither accumulation nor increased clearance with repeat dosing of STO-609 (Figure 6C). STO-609 was easily detected in tumour samples with a mean concentration of 2670 and 682 nM at 0.5 and 2 h, respectively (Figure 6C; Supplementary Figure S10). The tumour levels of STO-609 were approximately equal in tumour and plasma at 2 h (682 versus 663 nM, respectively), although earlier time points suggest that the tumour kinetics of STO-609 differ from plasma kinetics (Supplementary Figure S10). The growth of C4-2B prostate cancer xenografts was reduced in mice treated with the CAMKK2 inhibitor STO-609 (Figure 6D–F; Supplementary Figure S10) and we observed an additive effect with AR inhibition, in castrated mice treated with the CAMKK2 inhibitor STO-609 (Figure 6F). Interestingly, CAMKK2 inhibition had no measurable effect on normal mouse prostate size or the cytoplasmic volume of prostate epithelial cells (Supplementary Figure S10), whereas castration resulted in macroscopic loss of prostate size and atrophy of luminal epithelial cells (Supplementary Figure S10). This shows greater selective effects on cancer tissue through targeting CAMKK2 than through complete inhibition of the AR itself. Yet more significantly CAMKK2 is overexpressed in both hormone-sensitive and castrate-resistant prostate cancer, opening up the possibility of using CAMKK2 inhibitors alone or in combination with other therapies at all stages of the disease.

Discussion

Over the last 5 years a number of groups have employed ChIP to map genomic binding sites for the AR as a stepping stone to explain the contribution of the AR to prostate cancer (Jariwala *et al*, 2007; Massie *et al*, 2007; Takayama *et al*, 2007; Wang *et al*, 2007, 2009; Jia *et al*, 2008). These studies have provided important insights into the mechanisms which direct AR signalling (e.g., FOXA1 as an AR pioneer factor) and have identified castrate-resistant disease-specific AR signalling changes (e.g., UBE2C as an AR target only in castrate-resistant prostate cancer) (Wang *et al*, 2007, 2009; Jia *et al*, 2008). By contrast our approach has been to define AR transcriptional networks in distinct models of prostate cancer, defining actively transcribed target genes as those to which the AR and RNAP II are dynamically recruited in response to AR activation. In combination with the most detailed androgen-stimulated gene expression time course we have maximized the number of transcriptional events that have been captured and can be integrated with our ChIP data.

The enriched pathways in this core set of direct AR-regulated genes included cell-cycle and metabolic regulators. Metabolism is the biological process that can be most readily measured and studied in an experimental setting given the 50+ years of clinical biochemistry underpinning

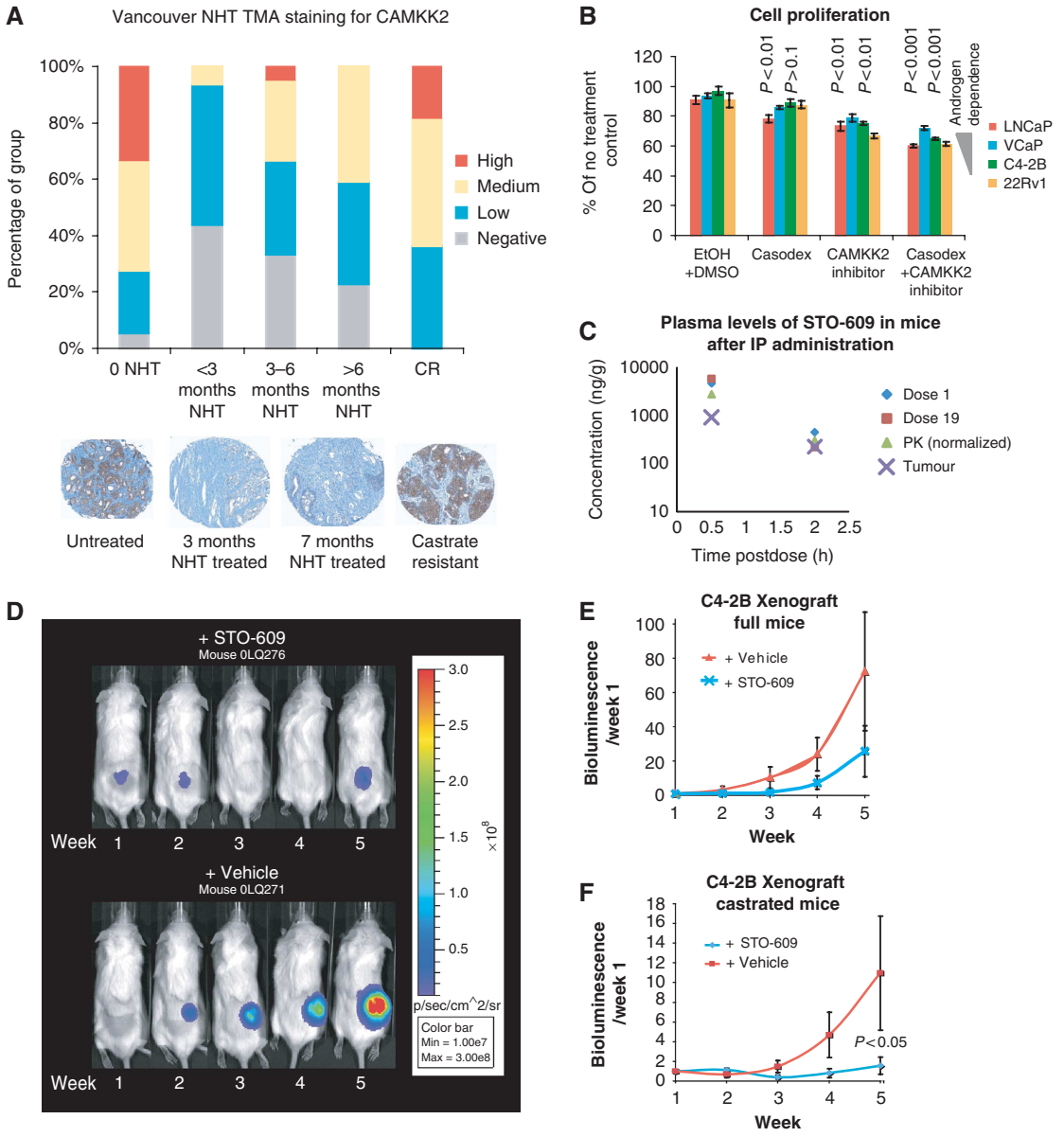

Figure 6 CAMKK2 expression and function under castrate conditions and in castrate-resistant prostate cancer. (**A**) Summary of CAMKK2 immunohistochemical (IHC) staining of a Neoadjuvant Hormone Therapy (NHT) tissue microarray (Vancouver NHT TMA) containing samples from hormone naive (0 NHT), NHT for <3 months, 3–6 months or >6 months and castrate-resistant prostate cancer (CR; as indicated; $n = 107$ cores). Representative images of CAMKK2 staining from untreated, 3 and 7 month-treated and castrate-resistant prostate cancer TMA cores. (**B**) Cell proliferation of LNCaP, VCaP, C4-2B and 22Rv1 cells 72 h following treatment with AR antagonist (10 μM casodex), CAMKK2 inhibitor (25 μM STO-609) or the combined treatment, as indicated (represented as percentage of untreated control, average of triplicate experiments ± s.e.m.). (**C**) Plasma and tumour levels of the CAMKK2 inhibitor STO-609 following intraperitoneal (IP) injection in C4-2B xenografted mice. Plasma harvested after the first treatment (dose 1), after the 19th treatment (dose 19), normalized pharmacokinetic (PK) and tumour measurements of STO-609 were quantified using mass spectroscopy (LC-MS/MS) relative to standard curve measurements. (**D**) Images of bioluminescent C4-2B xenograft tumours measured on week 1–5 from a single representative mouse from each treatment group. Mice were injected intraperitoneally three times per week with 10 μmol/kg of STO-609 or DMSO control (as indicated) and the growth of the tumours was monitored weekly using luciferase bioluminescence imaging. (**E**, **F**) Growth curve of bioluminescent C4-2B prostate cancer cell line xenografts ($n = 4$ per group). Full (**E**) and castrated (**F**) mice were treated with the CAMKK2 inhibitor STO-609 (10 μmol/kg) or vehicle control (DMSO) three times per week and imaged once per week following IP injection of 150 mg/kg luciferin. Expressed as bioluminescence relative to week 1 for each mouse (represented as mean ± s.e.m.).

our understanding of glycolysis and oxidative phosphorylation. Mounting evidence supports the addiction of cancer cells to aerobic glycolysis (Warburg effect) as a potential Achilles Heel for the treatment of cancer (Christofk *et al*, 2008; Tong *et al*, 2009; Vander Heiden *et al*, 2010). Consequently, we used metabolic pathways as a test-bed to prove that transcriptional biology can guide the biochemical study of prostate cancer.

Our combined analysis highlighted enzymes which regulate glycolytic flux (e.g., HK1 and HK2; 6-phosphofructo-2-kinase/fructose-2,6-biphosphatase 2, PFKFB2) and also enzymes which utilize glycolysis metabolites in the production

of lipids (e.g., FASN and ACACA) and nucleotides (e.g., the ADP-ribose diphosphatase NUDT9). This highlighted an anabolic program downstream of the AR in prostate cancer cells. Using multiple metabolomic approaches, we confirmed that AR signalling stimulates aerobic glycolysis and anabolism in prostate cancer cells.

We further refined the core set of direct AR target genes by undertaking a meta-analysis of clinical expression data to identify the downstream targets of the AR which are relevant to clinical disease. Only by integrating these distinct data sets we were able to identify CAMKK2, which otherwise was only one among hundreds of genes in our core AR-regulated gene set or reported to be overexpressed in prostate cancer. We discovered that CAMKK2 is a key effector of the AR, regulating glycolytic flux by activating AMPK-PFK signalling, which in turn drives anabolism and thereby controls prostate cancer cell proliferation and tumour growth.

The role of AMPK in prostate cancer is controversial (Park *et al*, 2009; Zhou *et al*, 2009); however, AMPK has an essential energy sensing role in cells and is critical in determining cell fate under stress conditions (Liang *et al*, 2007). Therefore, the timing, level and cellular context of AMPK activation may have profound effects on the functional consequences of AMPK signalling. For example, in normal somatic cells AMPK has been shown to activate glycolysis via PFK and inhibit protein biosynthesis by decreasing MTOR activity (Marsin *et al*, 2000; Gwinn *et al*, 2008). In contrast, our data indicate that CAMKK2 enhances metabolic flux by stimulating AMPK phosphorylation without any effect on mTOR activity. The mechanisms underlying this skewing of AMPK signalling in this context are unclear; however, it is possible that other targets of the AR or CAMKK2 may impact on these downstream pathways. The functional consequences of this signalling axis are clear from our functional studies which point to a role for CAMKK2 inhibitors as inducers of metabolic stress, sensitizing prostate cancer cells to the effects of AR antagonists and metabolic drugs.

In conclusion, our genomics study has uncovered a coordinated network of transcriptional changes orchestrated by the AR which includes upregulation of (1) glucose uptake and glycolysis (e.g., GLUT1, HK1/2 and PFKFB2); (2) biosynthetic pathways (e.g., FASN and ACACA); (3) master regulators of these metabolic processes (e.g., MTOR and CAMKK2); and (4) cell-cycle regulators (e.g., CDC2 and CDC25A). By taking an unbiased, interdisciplinary approach we confirmed the functional consequences of these transcriptional changes, finding that the AR enhances aerobic glycolysis and anabolic pathways which utilize glucose as a carbon source. Our functional data show that CAMKK2 has an essential role in regulating anabolic metabolism downstream of the AR in prostate cancer cells. In the course of preparing this manuscript another group reproduced our finding that CAMKK2 is an important downstream effector of the AR, selecting CAMKK2 from published expression array data on a candidate basis (Frigo *et al*, 2010). This study reported that CAMKK2 can also affect cell migration through a mechanism that has yet to be defined. A complete understanding of the function of CAMKK2 in prostate cancer will clearly depend on improved *in vivo* and *in vitro* models. However, our work provides a framework for future studies by defining the crucial role of CAMKK2 in anabolic metabolism, cell proliferation and as an important effector of AR signalling.

Materials and methods

Chromatin immunoprecipitation

ChIP was performed as previously described (Massie *et al*, 2007; Schmidt *et al*, 2008; Wilson *et al*, 2008) (see Supplementary data for details). Cells were cultured in phenol red-free RPMI media supplemented with 10% charcoal dextran-stripped FBS for 72 h before adding 1 nM R1881 or 0.01% ethanol for 4 h. AR and RNAP II antibodies used for ChIP were AR N20 (SC-816X, Santa Cruz) and phospho-Ser-5 RNAP II (AB-5401, Abcam). ChIP enrichment was tested by real-time PCR and the remainder was used for single-end SOLEXA library preparation.

ChIP-seq SOLEXA library preparation

Single-end SOLEXA sequencing libraries were prepared as previously described (Schmidt *et al*, 2008) (see Supplementary data for details). Sequence reads were generated using an Illumina (Solexa) Genome Analyzer II and these reads were mapped back to the reference human genome before peak calling.

Sequence read analysis

Sequence reads were generated by the Illumina analysis pipeline versions 1.3.4 and 1.4.0. The two lanes of reads were combined for each sample, and aligned to the Human Reference Genome (assembly hg18, NCBI Build 36.1, March 2008) using MAQ (Li *et al*, 2008). Next, they were filtered by alignment quality score, removing all reads with a MAQ score <20, and exact duplicate reads were removed such that no single read start position was represented more than once. Enriched regions of the genome were identified by comparing the ChIPed samples with input samples using two independent peak calling algorithms: MACS (Zhang *et al*, 2008) and ChIPSeqMini (Johnson *et al*, 2007), taking only those regions found by both algorithms. Sites found in the androgen-stimulated condition, but not the vehicle-treated condition, were taken forward for further analysis. All ChIP-seq data have been deposited at the NCBI Short Read Archive (SRA012454.1) and identified binding sites (peaks) are available in Supplementary Tables S1–S3. The 'super-set' of AR binding sites (Supplementary Table S3) was generated by combining the publicly available AR peak regions from previous reports (Horie-Inoue *et al*, 2004, 2006; Barski *et al*, 2007; Bolton *et al*, 2007; Jariwala *et al*, 2007; Massie *et al*, 2007; Takayama *et al*, 2007; Jia *et al*, 2008; Lin *et al*, 2009; Wang *et al*, 2009).

Analysis of ChIP peak regions

Overlap, subtraction, union and feature annotation of ChIP-seq enriched regions were performed using the Galaxy suite (Blankenberg *et al*, 2007; Taylor *et al*, 2007). Transcription factor motifs were identified using CEAS, *de novo* motif searches using MEME and Nested MICA (Bailey and Elkan, 1995; Down and Hubbard, 2005) and position weight matrix searches using RSAT matrix-scan (http://rsat.ulb.ac.be/rsat/). Motifs identified using *de novo* searches were aligned with known transcription factor PWMs using the motif alignment tool in the JASPAR database (http://jaspar.cgb.ki.se/). The optimal genomic distance between AR binding sites (peak boundaries) and androgen-regulated genes (gene boundaries) was defined using GSEA. Briefly, we generated gene sets by identifying all genes within 1, 2.5, 5, 25, 100, 200 and 500 kb of AR binding sites and control set were generated by identifying genes with no adjacent AR binding sites. These gene sets were tested for enrichment of the 3319 androgen-regulated genes identified in our detailed expression profiling data using GSEA (using the 'time course' correlation).

Illumina beadarrays

Forty-eight total RNA samples were harvested from LNCaP cells grown for 72 h in steroid depleted medium (RPMI supplemented with 10% charcoal dextran-stripped FBS). These comprised 3 time zero samples; 10 vehicle (ethanol) control samples taken at 2, 4, 8, 12 and 24 h in duplicate; 36 androgen (R1881)-treated samples taken every 30 min for 4 h then every hour until 24 h following treatment (with replicates at 1, 2, 4, 8, 12, 16, 20 and 24 h).

Autocorrelation analysis of Illumina gene expression data

The Illumina HumanWG v2 BeadArrays consist of two replicate sections that we treat as technical replicate arrays for the purposes

of this analysis due to small but systematic shifts between sections that need to be addressed in the normalization. Data were analysed from the raw bead-level using the beadarray software, with spatial artefacts identified and removed automatically (BASH) and curated manually (Dunning *et al*, 2007; Cairns *et al*, 2008). The resultant, reduced, data set was then summarized in a standard manner (with outliers removed) in order to obtain a mean log-intensity and standard error for each probe/array combination. The November 2008 annotation from http://www.compbio.group.cam.ac.uk/Resources/Annotation/index.html was used to map probes to transcripts, and probes with no 'good' or 'perfect' match were discarded along with those that registered no signal above background on all 96 arrays. This resulted in 17 182 probes for which analysis proceeded.

To detect probes that showed a systematic, smooth, change over time without prescribing a form for that change we used the autocorrelation at lag 1 as a measure of activity. This measure identifies profiles where neighbouring time points are more similar than disparate time points, and so can identify all smooth and systematic gene expression changes regardless of the shapes of their profiles. To account for the uncertainty in our measurements, we simulated 100 sets of observations from the known mean values and standard errors, calculated the autocorrelation of each and took the mean. Simulations and arguments of symmetry suggested that a cutoff of autocorrelation 0.5 would lead to a low false-discovery rate and 4224 probes passed this threshold. Raw and normalized data from Illumina BeadArray experiments have been deposited at GEO (under accession GSE18684).

Functional annotation was done using the DAVID gene ontology tool, GSEA and interaction networks were generated using Cytoscape with the BiNGO and BioNetBuilder plug-ins.

Real-time PCR validation

We used SYBR-green quantitative real-time PCR to confirm AR binding sites and gene expression changes (see Supplementary data for details and primer sequences).

Immunohistochemistry

Tissue sections were stained with CAMKK2 antibody (Atlas Antibodies #HPA017389) at a 1:100 dilution (see Supplementary data for details).

Xenograft experiments

Xenograft tumours were generated with C4-2b cells that stably expressed a fusion protein of luciferase and YFP. There were four groups of mice (castration + vehicle, castration + STO-609, full + vehicle and full + STO-609), each consisting of four mice. In all, 10 μmol/kg of STO-609 (or the equivalent vehicle, 10% DMSO in PBS) was injected intraperitoneally three times per week and the growth of the tumours was monitored weekly through bioluminescence with an IVIS camera (Xenogen). See Supplementary data for details.

Pharmacokinetic/pharmacodynamic measurements

For plasma studies, mice (Supplementary Figure S10B) were injected IV or IP with 0.5 μmol/kg STO-609 and at time points (5, 15, 30, 45 min, 1, 1.5, 2, 4, 6 h) after treatment blood samples were collected into heparinized tubes. Blood was centrifuged to obtain the plasma fraction and frozen at −80°C before analysis. For tumour and parallel serum measurements (Figure 6C), mice were treated with 10 μmol/kg and samples of blood and tumour were collected at 0.5 and 2 h after treatment. Bioanalysis was carried out by protein precipitation of plasma followed by detection using an STO-609-specific LC-MS/MS method with an assay range of 1–1000 ng/ml. The plasma concentration:time profile was then constructed for PK analysis by WinNonLin. Tumour samples were homogenized 4 v/w in 50% CH_3CN (aq). An aliquot of this homogenate then processed using the same extraction procedure as plasma. The assay range for STO609 in tumour homogenate was 4–4000 ng/g.

Metabolomic profiling

LNCaP cells grown in RPMI media supplemented with 10% FBS were harvested on days 0, 1, 2 and 3 after DMSO or STO-609 treatment. LNCaP cells grown in RPMI media supplemented with 10% charcoal dextran-treated (steroid depleted) FBS were harvested on days 0, 1, 2 and 3 with and without androgen treatment (1 nM R1881). Cell culture media and cell lysates were collected from all the cell plates for NMR analysis. ^{1}H NMR spectroscopy data were acquired on a 600 MHz Bruker Avance NMR spectrometer. See Supplementary data for details. Metabolite concentrations were normalized to the protein content of cells.

Glucose flux experiments using 1,2-13C2-glucose and GC/MS

Cells were grown in media supplemented with charcoal dextran-treated FBS (steroid depleted conditions) and treated either with vehicle (0.01% ethanol), androgen (1 nM R1881), androgen + STO-609 (25 μM) or androgen + CAMKK2 siRNA for 72 h. Cells were harvested by scraping on ice and metabolites were obtained by methanol/chloroform extraction (Wu *et al*, 2008). The aqueous phase was dried using a Speedvac and derivatized by silylation (Perroud *et al*, 2006). RNA ribose extraction and derivatization was performed as previously described (Boren *et al*, 2003). The sample was injected into a GC-TOF MS (Leco Pegasus HT GC/TOFMS; Leco UK, Stockport, UK) and run according to methods described previously (Perroud *et al*, 2006). The obtained chromatograms were analysed using the ChromaTOF software package (Leco UK) to identify the different peaks. Mass spectral results were accepted only if the standard sample deviation was <1% of the normalized peak intensity.

PFK activity measurements

PFK activity was measured in prostate cancer cell line extracts using the method of Brand and Soling (1974), see Supplementary data for details.

Glucose and lactate measurements

Media were harvested from cells grown in RPMI supplemented with either 10% FBS or 10% charcoal dextran-treated FBS and treated for 3 days with or without androgen, bicalutamide (casodex) or ST0-609. Glucose and lactate levels were determined using commercial enzyme based kits (Abcam and BioVision Inc., USA).

Oxygen consumption

Oxygen consumption of cell suspensions was measured using a Clark-type oxygen electrode (DW1 Oxygen Electrode Chamber, Hansatech) over a 15 min time course at 37°C, according to the manufacturer's instructions (see Supplementary data for details).

Supplementary data

Supplementary data are available at *The EMBO Journal* Online (http://www.embojournal.org).

Acknowledgements

We are grateful to study volunteers for their participation and to staff at the Wellcome Trust Clinical Research Facility, Addenbrooke's Clinical Research Centre, Cambridge for their help in conducting the study. We also acknowledge the support of the NIHR Cambridge Biomedical Research Centre, the DOH HTA (ProtecT grant) and the MRC (ProMPT grant). We are also grateful for the support, materials and constructive input from Jason Carroll and his lab. This work was funded by a CRUK program grant awarded to DEN. We acknowledge the support of The University of Cambridge, Cancer Research UK and Hutchison Whampoa Limited. All expression array data (GSE18684) and ChIP-seq data (GSE28126 and SRA012454.1) have been deposited at GEO and SRA.

Author contributions: CEM designed the study, wrote the manuscript and was involved in all aspects of the project; AL applied autocorrelation analysis to expression profiling data and analysed other genomics data; ARM designed and performed xenograft experiments and PFK activity measurements; JB designed and carried out GC/MS studies; RS analysed ChIP-seq data; LF scored CAMKK2 IHC staining and provided tissue microarrays; AW scored CAMKK2 IHC staining and provided tissue microarrays; HS carried out xenograft experiments and IHC staining; BM designed and carried out 1H NMR studies; NS performed ChIP from human samples; HB carried out FACS analysis; VZ carried out IF staining; DMS carried out PK measurements for xenograft experiments; GMD designed and set-up oxygen consumption protocols; NM

carried out Illumina sequencing; MO processed expression arrays; JH processed expression arrays; SM provided bioinformatics support; BM carried out motif analysis; SKL designed and set-up xenograft models; KMB designed luciferase xenograft models and GC/MS experiments; JG designed and evaluated 1H NMR experiments; MG and PR provided tissue microarrays; DEN designed the study and wrote the manuscript; IM designed the study and wrote the manuscript.

Conflict of interest

The authors declare that they have no conflict of interest.

References

Anderson KA, Ribar TJ, Lin F, Noeldner PK, Green MF, Muehlbauer MJ, Witters LA, Kemp BE, Means AR (2008) Hypothalamic CaMKK2 contributes to the regulation of energy balance. *Cell Metab* **7:** 377–388

Attar RM, Jure-Kunkel M, Balog A, Cvijic ME, Dell-John J, Rizzo CA, Schweizer L, Spires TE, Platero JS, Obermeier M, Shan W, Salvati ME, Foster WR, Dinchuk J, Chen SJ, Vite G, Kramer R, Gottardis MM (2009) Discovery of BMS-641988, a novel and potent inhibitor of androgen receptor signaling for the treatment of prostate cancer. *Cancer Res* **69:** 6522–6530

Attard G, Reid AH, A'Hern R, Parker C, Oommen NB, Folkerd E, Messiou C, Molife LR, Maier G, Thompson E, Olmos D, Sinha R, Lee G, Dowsett M, Kaye SB, Dearnaley D, Kheoh T, Molina A, de Bono JS (2009) Selective inhibition of CYP17 with abiraterone acetate is highly active in the treatment of castration-resistant prostate cancer. *J Clin Oncol* **27:** 3742–3748

Bailey TL, Elkan C (1995) The value of prior knowledge in discovering motifs with MEME. *Proc Int Conf Intell Syst Mol Biol* **3:** 21–29

Barski A, Cuddapah S, Cui K, Roh TY, Schones DE, Wang Z, Wei G, Chepelev I, Zhao K (2007) High-resolution profiling of histone methylations in the human genome. *Cell* **129:** 823–837

Bernstein BE, Mikkelsen TS, Xie X, Kamal M, Huebert DJ, Cuff J, Fry B, Meissner A, Wernig M, Plath K, Jaenisch R, Wagschal A, Feil R, Schreiber SL, Lander ES (2006) A bivalent chromatin structure marks key developmental genes in embryonic stem cells. *Cell* **125:** 315–326

Blankenberg D, Taylor J, Schenck I, He J, Zhang Y, Ghent M, Veeraraghavan N, Albert I, Miller W, Makova KD, Hardison RC, Nekrutenko A (2007) A framework for collaborative analysis of ENCODE data: making large-scale analyses biologist-friendly. *Genome Res* **17:** 960–964

Bolton EC, So AY, Chaivorapol C, Haqq CM, Li H, Yamamoto KR (2007) Cell- and gene-specific regulation of primary target genes by the androgen receptor. *Genes Dev* **21:** 2005–2017

Boren J, Lee W-NP, Bassilian S, Centelles JJ, Lim S, Ahmed S, Boros LG, Cascante M (2003) The stable isotope-based dynamic metabolic profile of butyrate-induced HT29 cell differentiation. *J Biol Chem* **278:** 28395–28402

Brand IA, Soling HD (1974) Rat liver phosphofructokinase. Purification and characterization of its reaction mechanism. *J Biol Chem* **249:** 7824–7831

Cairns JM, Dunning MJ, Ritchie ME, Russell R, Lynch AG (2008) BASH: a tool for managing BeadArray spatial artefacts. *Bioinformatics* **24:** 2921–2922

Carroll JS, Meyer CA, Song J, Li W, Geistlinger TR, Eeckhoute J, Brodsky AS, Keeton EK, Fertuck KC, Hall GF, Wang Q, Bekiranov S, Sementchenko V, Fox EA, Silver PA, Gingeras TR, Liu XS, Brown M (2006) Genome-wide analysis of estrogen receptor binding sites. *Nat Genet* **38:** 1289–1297

Chen C, Sun X, Guo P, Dong XY, Sethi P, Zhou W, Zhou Z, Petros J, Frierson Jr HF, Vessella RL, Atfi A, Dong JT (2007) Ubiquitin E3 ligase WWP1 as an oncogenic factor in human prostate cancer. *Oncogene* **26:** 2386–2394

Christofk HR, Vander Heiden MG, Harris MH, Ramanathan A, Gerszten RE, Wei R, Fleming MD, Schreiber SL, Cantley LC (2008) The M2 splice isoform of pyruvate kinase is important for cancer metabolism and tumour growth. *Nature* **452:** 230–233

Core LJ, Waterfall JJ, Lis JT (2008) Nascent RNA sequencing reveals widespread pausing and divergent initiation at human promoters. *Science (New York, NY)* **322:** 1845–1848

Costello LC, Liu Y, Franklin RB, Kennedy MC (1997) Zinc inhibition of mitochondrial aconitase and its importance in citrate metabolism of prostate epithelial cells. *J Biol Chem* **272:** 28875–28881

Craft N, Shostak Y, Carey M, Sawyers CL (1999) A mechanism for hormone-independent prostate cancer through modulation of androgen receptor signaling by the HER-2/neu tyrosine kinase. *Nat Med* **5:** 280–285

Down TA, Hubbard TJ (2005) NestedMICA: sensitive inference of over-represented motifs in nucleic acid sequence. *Nucleic Acids Res* **33:** 1445–1453

Dunning MJ, Smith ML, Ritchie ME, Tavare S (2007) Beadarray: R classes and methods for Illumina bead-based data. *Bioinformatics* **23:** 2183–2184

Frigo DE, Howe MK, Wittmann BM, Brunner AM, Cushman I, Wang Q, Brown M, Means AR, McDonnell DP (2010) CaM Kinase Kinase {beta}-mediated activation of the growth regulatory kinase AMPK is required for androgen-dependent migration of prostate cancer cells. *Cancer Res* **71:** 528–537

Gwinn DM, Shackelford DB, Egan DF, Mihaylova MM, Mery A, Vasquez DS, Turk BE, Shaw RJ (2008) AMPK phosphorylation of raptor mediates a metabolic checkpoint. *Mol Cell* **30:** 214–226

Haag P, Bektic J, Bartsch G, Klocker H, Eder IE (2005) Androgen receptor down regulation by small interference RNA induces cell growth inhibition in androgen sensitive as well as in androgen independent prostate cancer cells. *J Steroid Biochem Mol Biol* **96:** 251–258

Hara T, Miyazaki H, Lee A, Tran CP, Reiter RE (2008) Androgen receptor and invasion in prostate cancer. *Cancer Res* **68:** 1128–1135

Heemers H, Maes B, Foufelle F, Heyns W, Verhoeven G, Swinnen JV (2001) Androgens stimulate lipogenic gene expression in prostate cancer cells by activation of the sterol regulatory element-binding protein cleavage activating protein/sterol regulatory element-binding protein pathway. *Mol Endocrinol (Baltimore, Md)* **15:** 1817–1828

Heemers H, Verrijdt G, Organe S, Claessens F, Heyns W, Verhoeven G, Swinnen JV (2004) Identification of an androgen response element in intron 8 of the sterol regulatory element-binding protein cleavage-activating protein gene allowing direct regulation by the androgen receptor. *J Biol Chem* **279:** 30880–30887

Hellawell GO, Turner GD, Davies DR, Poulsom R, Brewster SF, Macaulay VM (2002) Expression of the type 1 insulin-like growth factor receptor is up-regulated in primary prostate cancer and commonly persists in metastatic disease. *Cancer Res* **62:** 2942–2950

Horie-Inoue K, Bono H, Okazaki Y, Inoue S (2004) Identification and functional analysis of consensus androgen response elements in human prostate cancer cells. *Biochem Biophys Res Commun* **325:** 1312–1317

Horie-Inoue K, Takayama K, Bono HU, Ouchi Y, Okazaki Y, Inoue S (2006) Identification of novel steroid target genes through the combination of bioinformatics and functional analysis of hormone response elements. *Biochem Biophys Res Commun* **339:** 99–106

Jariwala U, Prescott J, Jia L, Barski A, Pregizer S, Cogan JP, Arasheben A, Tilley WD, Scher HI, Gerald WL, Buchanan G, Coetzee GA, Frenkel B (2007) Identification of novel androgen receptor target genes in prostate cancer. *Mol Cancer* **6:** 39

Jia L, Berman BP, Jariwala U, Yan X, Cogan JP, Walters A, Chen T, Buchanan G, Frenkel B, Coetzee GA (2008) Genomic androgen receptor-occupied regions with different functions, defined by histone acetylation, coregulators and transcriptional capacity. *PLoS One* **3:** e3645

Jiang Z, Woda BA, Rock KL, Xu Y, Savas L, Khan A, Pihan G, Cai F, Babcook JS, Rathanaswami P, Reed SG, Xu J, Fanger GR (2001) P504S: a new molecular marker for the detection of prostate carcinoma. *Am J Surg Pathol* **25:** 1397–1404

Jiang Z, Woda BA, Yang XJ (2002) Alpha-methylacyl coenzyme A racemase as a marker for prostate cancer. *JAMA* **287:** 3080–3081; author reply 3081

Johnson DS, Mortazavi A, Myers RM, Wold B (2007) Genome-wide mapping of *in vivo* protein-DNA interactions. *Science (New York, NY)* **316:** 1497–1502

Knudsen KE, Arden KC, Cavenee WK (1998) Multiple G1 regulatory elements control the androgen-dependent proliferation of prostatic carcinoma cells. *J Biol Chem* **273:** 20213–20222

Li H, Ruan J, Durbin R (2008) Mapping short DNA sequencing reads and calling variants using mapping quality scores. *Genome Res* **18:** 1851–1858

Liang J, Shao SH, Xu ZX, Hennessy B, Ding Z, Larrea M, Kondo S, Dumont DJ, Gutterman JU, Walker CL, Slingerland JM, Mills GB (2007) The energy sensing LKB1-AMPK pathway regulates p27(kip1) phosphorylation mediating the decision to enter autophagy or apoptosis. *Nat Cell Biol* **9:** 218–224

Lin B, Wang J, Hong X, Yan X, Hwang D, Cho JH, Yi D, Utleg AG, Fang X, Schones DE, Zhao K, Omenn GS, Hood L (2009) Integrated expression profiling and ChIP-seq analyses of the growth inhibition response program of the androgen receptor. *PLoS One* **4:** e6589

Makkonen H, Kauhanen M, Jaaskelainen T, Palvimo JJ (2011) Androgen receptor amplification is reflected in the transcriptional responses of vertebral-cancer of the prostate cells. *Mol Cell Endocrinol* **331:** 57–65

Margiotti K, Wafa LA, Cheng H, Novelli G, Nelson CC, Rennie PS (2007) Androgen-regulated genes differentially modulated by the androgen receptor coactivator L-dopa decarboxylase in human prostate cancer cells. *Mol Cancer* **6:** 38

Marsin AS, Bertrand L, Rider MH, Deprez J, Beauloye C, Vincent MF, Van den Berghe G, Carling D, Hue L (2000) Phosphorylation and activation of heart PFK-2 by AMPK has a role in the stimulation of glycolysis during ischaemia. *Curr Biol* **10:** 1247–1255

Massie CE, Adryan B, Barbosa-Morais NL, Lynch AG, Tran MG, Neal DE, Mills IG (2007) New androgen receptor genomic targets show an interaction with the ETS1 transcription factor. *EMBO Rep* **8:** 871–878

Mehta PB, Jenkins BL, McCarthy L, Thilak L, Robson CN, Neal DE, Leung HY (2003) MEK5 overexpression is associated with metastatic prostate cancer, and stimulates proliferation, MMP-9 expression and invasion. *Oncogene* **22:** 1381–1389

Migita T, Ruiz S, Fornari A, Fiorentino M, Priolo C, Zadra G, Inazuka F, Grisanzio C, Palescandolo E, Shin E, Fiore C, Xie W, Kung AL, Febbo PG, Subramanian A, Mucci L, Ma J, Signoretti S, Stampfer M, Hahn WC *et al* (2009) Fatty acid synthase: a metabolic enzyme and candidate oncogene in prostate cancer. *J Natl Cancer Inst* **101:** 519–532

Mootha VK, Lindgren CM, Eriksson KF, Subramanian A, Sihag S, Lehar J, Puigserver P, Carlsson E, Ridderstrale M, Laurila E, Houstis N, Daly MJ, Patterson N, Mesirov JP, Golub TR, Tamayo P, Spiegelman B, Lander ES, Hirschhorn JN, Altshuler D *et al* (2003) PGC-1alpha-responsive genes involved in oxidative phosphorylation are coordinately downregulated in human diabetes. *Nat Genet* **34:** 267–273

Park HU, Suy S, Danner M, Dailey V, Zhang Y, Li H, Hyduke DR, Collins BT, Gagnon G, Kallakury B, Kumar D, Brown ML, Fornace A, Dritschilo A, Collins SP (2009) AMP-activated protein kinase promotes human prostate cancer cell growth and survival. *Mol Cancer Ther* **8:** 733–741

Perroud B, Lee J, Valkova N, Dhirapong A, Lin PY, Fiehn O, Kultz D, Weiss RH (2006) Pathway analysis of kidney cancer using proteomics and metabolic profiling. *Mol Cancer* **5:** 64

Prescott J, Jariwala U, Jia L, Cogan JP, Barski A, Pregizer S, Shen HC, Arasheben A, Neilson JJ, Frenkel B, Coetzee GA (2007) Androgen receptor-mediated repression of novel target genes. *Prostate* **67:** 1371–1383

Rhodes DR, Yu J, Shanker K, Deshpande N, Varambally R, Ghosh D, Barrette T, Pandey A, Chinnaiyan AM (2004) ONCOMINE: a cancer microarray database and integrated data-mining platform. *Neoplasia* **6:** 1–6

Roche PJ, Hoare SA, Parker MG (1992) A consensus DNA-binding site for the androgen receptor. *Mol Endocrinol (Baltimore, Md)* **6:** 2229–2235

Schmidt D, Stark R, Wilson MD, Brown GD, Odom DT (2008) Genome-scale validation of deep-sequencing libraries. *PLoS One* **3:** e3713

Sherk AB, Frigo DE, Schnackenberg CG, Bray JD, Laping NJ, Trizna W, Hammond M, Patterson JR, Thompson SK, Kazmin D, Norris JD, McDonnell DP (2008) Development of a small-molecule serum- and glucocorticoid-regulated kinase-1 antagonist and its evaluation as a prostate cancer therapeutic. *Cancer Res* **68:** 7475–7483

Snoek R, Cheng H, Margiotti K, Wafa LA, Wong CA, Wong EC, Fazli L, Nelson CC, Gleave ME, Rennie PS (2009) *In vivo* knockdown of the androgen receptor results in growth inhibition and regression of well-established, castration-resistant prostate tumors. *Clin Cancer Res* **15:** 39–47

Steinkamp MP, O'Mahony OA, Brogley M, Rehman H, Lapensee EW, Dhanasekaran S, Hofer MD, Kuefer R, Chinnaiyan A, Rubin MA, Pienta KJ, Robins DM (2009) Treatment-dependent androgen receptor mutations in prostate cancer exploit multiple mechanisms to evade therapy. *Cancer Res* **69:** 4434–4442

Takayama K, Kaneshiro K, Tsutsumi S, Horie-Inoue K, Ikeda K, Urano T, Ijichi N, Ouchi Y, Shirahige K, Aburatani H, Inoue S (2007) Identification of novel androgen response genes in prostate cancer cells by coupling chromatin immunoprecipitation and genomic microarray analysis. *Oncogene* **26:** 4453–4463

Taylor J, Schenck I, Blankenberg D, Nekrutenko A (2007) Using galaxy to perform large-scale interactive data analyses. *Curr Protoc Bioinformatics* **19:** 10.5.1–10.5.25

Tokumitsu H, Inuzuka H, Ishikawa Y, Ikeda M, Saji I, Kobayashi R (2002) STO-609, a specific inhibitor of the Ca(2+)/calmodulin-dependent protein kinase kinase. *J Biol Chem* **277:** 15813–15818

Tong X, Zhao F, Mancuso A, Gruber JJ, Thompson CB (2009) The glucose-responsive transcription factor ChREBP contributes to glucose-dependent anabolic synthesis and cell proliferation. *Proc Natl Acad Sci USA* **106:** 21660–21665

Tran C, Ouk S, Clegg NJ, Chen Y, Watson PA, Arora V, Wongvipat J, Smith-Jones PM, Yoo D, Kwon A, Wasielewska T, Welsbie D, Chen CD, Higano CS, Beer TM, Hung DT, Scher HI, Jung ME, Sawyers CL (2009) Development of a second-generation antiandrogen for treatment of advanced prostate cancer. *Science (New York, NY)* **324:** 787–790

Vander Heiden MG, Cantley LC, Thompson CB (2009) Understanding the Warburg effect: the metabolic requirements of cell proliferation. *Science* **324:** 1029–1033

Vander Heiden MG, Locasale JW, Swanson KD, Sharfi H, Heffron GJ, Amador-Noguez D, Christofk HR, Wagner G, Rabinowitz JD, Asara JM, Cantley LC (2010) Evidence for an alternative glycolytic pathway in rapidly proliferating cells. *Science (New York, NY)* **329:** 1492–1499

Varambally S, Yu J, Laxman B, Rhodes DR, Mehra R, Tomlins SA, Shah RB, Chandran U, Monzon FA, Becich MJ, Wei JT, Pienta KJ, Ghosh D, Rubin MA, Chinnaiyan AM (2005) Integrative genomic and proteomic analysis of prostate cancer reveals signatures of metastatic progression. *Cancer Cell* **8:** 393–406

Velasco AM, Gillis KA, Li Y, Brown EL, Sadler TM, Achilleos M, Greenberger LM, Frost P, Bai W, Zhang Y (2004) Identification and validation of novel androgen-regulated genes in prostate cancer. *Endocrinology* **145:** 3913–3924

Veldscholte J, Ris-Stalpers C, Kuiper GG, Jenster G, Berrevoets C, Claassen E, van Rooij HC, Trapman J, Brinkmann AO, Mulder E (1990) A mutation in the ligand binding domain of the androgen receptor of human LNCaP cells affects steroid binding characteristics and response to anti-androgens. *Biochem Biophys Res Commun* **173:** 534–540

Visakorpi T, Hyytinen E, Koivisto P, Tanner M, Keinanen R, Palmberg C, Palotie A, Tammela T, Isola J, Kallioniemi OP (1995) *In vivo* amplification of the androgen receptor gene and progression of human prostate cancer. *Nat Genet* **9:** 401–406

Wang Q, Li W, Liu XS, Carroll JS, Janne OA, Keeton EK, Chinnaiyan AM, Pienta KJ, Brown M (2007) A hierarchical network of transcription factors governs androgen receptor-dependent prostate cancer growth. *Mol Cell* **27:** 380–392

Wang Q, Li W, Zhang Y, Yuan X, Xu K, Yu J, Chen Z, Beroukhim R, Wang H, Lupien M, Wu T, Regan MM, Meyer CA, Carroll JS, Manrai AK, Janne OA, Balk SP, Mehra R, Han B, Chinnaiyan AM *et al* (2009) Androgen receptor regulates a distinct transcription program in androgen-independent prostate cancer. *Cell* **138:** 245–256

Wilson MD, Barbosa-Morais NL, Schmidt D, Conboy CM, Vanes L, Tybulewicz VL, Fisher EM, Tavare S, Odom DT (2008) Species-specific transcription in mice carrying human chromosome 21. *Science (New York, NY)* **322:** 434–438

Wu H, Southam AD, Hines A, Viant MR (2008) High-throughput tissue extraction protocol for NMR- and MS-based metabolomics. *Anal Biochem* **372:** 204–212

Xu Y, Chen SY, Ross KN, Balk SP (2006) Androgens induce prostate cancer cell proliferation through mammalian target of rapamycin activation and post-transcriptional increases in cyclin D proteins. *Cancer Res* **66:** 7783–7792

Yu J, Mani RS, Cao Q, Brenner CJ, Cao X, Wang X, Wu L, Li J, Hu M, Gong Y, Cheng H, Laxman B, Vellaichamy A, Shankar S, Li Y, Dhanasekaran SM, Morey R, Barrette T, Lonigro RJ, Tomlins SA *et al* (2010) An integrated network of androgen receptor, polycomb, and TMPRSS2-ERG gene fusions in prostate cancer progression. *Cancer Cell* **17:** 443–454

Zhang Y, Liu T, Meyer CA, Eeckhoute J, Johnson DS, Bernstein BE, Nusbaum C, Myers RM, Brown M, Li W, Liu XS (2008) Model-based analysis of ChIP-Seq (MACS). *Genome Biol* **9:** R137

Zhou J, Huang W, Tao R, Ibaragi S, Lan F, Ido Y, Wu X, Alekseyev YO, Lenburg ME, Hu GF, Luo Z (2009) Inactivation of AMPK alters gene expression and promotes growth of prostate cancer cells. *Oncogene* **28:** 1993–2002